Facies Analysis and Permeability Estimation in Late Cretaceous Giant Carbonate Reservoir using LWD Technology: A Case Study in Sabriyah Field, North Kuwait*

Ahmed Elsherif[1], Kais Gzara[1], Hossam Ibrahim[2], and J. Krafft[2]

Search and Discovery Article #41842 (2016)**
Posted August 8, 2016

*Adapted from extended abstract based on oral presentation given at AAPG GEO 2016, The 12th Middle East Geosciences Conference and Exhibition March 7-10, 2016, Manama, Bahrain

[1]Schlumberger (KGzara@slb.com)
[2]Kuwait Oil Company

Abstract

The Sabriya Field Mauddud original development plan was based on an inverted 9 spot pattern to produce oil from multi-carbonate reservoir layers. Recently, Kuwait Oil Company (KOC) implemented a paradigm shift to an intensive campaign for drilling horizontal wells in the Mauddud Formation in North Kuwait. The lateral section extended for a long interval penetrating different facies of the Maudud carbonate reservoir. The need for advanced formation evaluation was highlighted as critical where the complex pore structure will play a big role in fluid mobility.

Formation mobility in carbonate reservoirs has been always a challenge in any formation evaluation. The Sabriya Mauddud Formation is a ramp system, ranging from shallow restricted and barrier shoal/rudist buildup to outer ramp sedimentation. The Mauddud carbonate is divided into two parts, a lower (Maj-MaG/F) belongs to outer to middle ramp dominated with intermittent influxes of Burgan delta shoreface sandstone sediments. The upper Mauddud (MaF to MaA) is inner ramp, barrier shoal/rudist build-up and shallow restricted packstone/grainstone facies. The best reservoir quality is in the inner/middle ramp and barrier shoal/rudist build-up facies of MaE, MaD, MaC, and MaB. The current strategy in Mauddud development plans is to produce high (MaB/MaC) and inject low (MaE/MaD).

The LWD resistivity was used in this field to measure resistivity (Laterolog type) to calculate water saturation. In addition, due to the fact that LWD tools measure while rotating, several resistivity images with different depths of investigation were also available in real time and recorded mode. In this case, the LWD resistivity imaging was used to study azimuthal formation porosity distribution in order to quantify the different porosity portions (Primary/Secondary). Following that, an empirical equation was used to determine formation permeability profile. This qualitative profile is calibrated to the formation pressure/mobility with high vertical resolution to enhance permeability calculations compared to derived permeability from standard open-hole logs.

Facies determinations were obtained based on porosity spectrum, amount of secondary porosity combined with relevant logging results using a neural network technique. This is significant to optimize well placement in the best reservoir rock types (grainstones, rudist build-up, and packstones). This has been proved as a successful technique for horizontal well ICD completion compartmentalization design.

Introduction to Sabirya Field

The Mid-Cretaceous Mauddud Formation is the main producing carbonate reservoir in the Raudhatain and Sabiriyah fields of northern Kuwait (Figure 1). Historical reservoir information and results from recent waterflood pilots indicate that reservoir performance in these reservoirs is controlled by geological complexity at several scales.

The carbonate-dominated Mauddud Formation overlies the Upper Burgan Member, a thick succession of fluvio-deltaic deposits, and consists of a diverse suite of carbonate facies deposited in low to high-energy shallow marine ramp settings (Figure 2). The basal part of the reservoir comprises mixed carbonate and siliciclastic sediments and reflects the establishment of a carbonate-dominated regime during waning supply of Burgan siliciclastic sediment.

This system was eventually drowned and covered by the Ahmadi Formation, a shaly offshore succession that is also the reservoir seal. Sedimentary facies associations and microfossil assemblages within the reservoir are organised in a broadly upward-shallowing succession constructed of several transgressive-regressive cycles which are defined by prominent, widely-correlatable flooding surfaces. Please refer to Figure 3 for depositional environments facies.

Each cycle exhibits a characteristic internal stacking pattern of minor depositional cycles. Fieldwide mapping and interpretation of facies within each cycle reveals a SW to NE, proximal to distal, trend consistent with regional seismic and palaeogeographic interpretations.

The high-energy, inner- to mid-ramp carbonate succession in the lower portion of the Mauddud reservoir is punctuated by siliciclastic incursions. Abrupt lateral facies changes, thickness variations, and local intra-reservoir erosion surfaces in this section suggest that deposition was influenced by subtle syndepositional tectonism. The upper part of the reservoir, in contrast, lacks significant siliciclastic influence and is made up of widely correlatable lower energy carbonate facies, although local subtle facies variations suggest that the Raudhatain-Sabiriyah structures continued as palaeohighs during deposition.

The contrast between grain-dominated facies at the crests of the two structures and muddier facies along the flanks was accentuated by carbonate cementation in the water legs of the reservoirs, largely in the form of calcite concretions of variable density. Cementation is most pronounced in low-energy wackestone facies, particularly in proximity to flooding surfaces where nodules may amalgamate to form laterally continuous, cemented layers. Another significant, but contrasting, diagenetic modification to the reservoir was the generation of secondary macroporosity by dissolution of aragonitic skeletal components.

The depositional evolution of the Mauddud reservoir, and its subsequent diagenetic overprint, created reservoir heterogeneities which exert a critical influence on reservoir performance; the most significant of these is the relationship between horizontal and vertical permeability.

Parasequences dominated by high-energy inner-ramp grainstones, thin inner-ramp rudist-bearing tempestites, and rudist biostromes constitute thief zones that represent challenges to reservoir management. In contrast, cemented layers and flooding surfaces support pressure differentials up to several hundred psi, thus complicating sweep and promoting reservoir compartmentalisation. The strong depositional control on the distribution of thief zones and intra-reservoir baffles demonstrates how important it is to comprehensively understand reservoir sedimentology and stratigraphy when devising long term development plans for reservoirs of this deceptively simple character.

Carbonate Reservoirs

It is estimated that more than 60% of the world's oil and 40% of the world's gas reserves are held in carbonate reservoirs. The Middle East, for example, is dominated by carbonate fields, with around 70% of oil and 90% of gas reserves held within these reservoirs (Figure 4).

Carbonates can exhibit highly varying properties (e.g. porosity, permeability, flow mechanisms) within small sections of the reservoir, making them difficult to characterize. A focused approach is needed to better understand the heterogeneous nature of the rock containing the fluids and the flow properties within the porous and often fractured formations. This involves detailed understanding of the fluids saturation, pore-size distribution, permeability, rock texture, reservoir rock type, and natural fracture systems at different scales.

The Carbonate Challenge

Carbonate reservoir rocks present several challenges that are different from challenges in clastic rocks. First, carbonate minerals are more chemically active than the minerals associated with sandstone reservoirs. Second, the poor correlation between porosity and permeability in carbonate rocks and the presence of fractures and other large scale heterogeneities can create very complex paths for fluid flow. This, in turn, makes it difficult for reservoir engineers to model the distribution of permeability in the carbonate reservoir models and predict production behavior.

All these factors make carbonate reservoirs more challenging in terms of reserves evaluation and reservoir modeling and simulation. Developing production strategies that will increase hydrocarbon recovery requires the combination of technologies and integration between several disciplines.

Carbonate Porosity

The porosity of carbonate rocks can be grouped into three types:

- Connected porosity, existing between carbonate grains.

- Vugs, which are unconnected pores resulting from the dissolution of calcite by water during diagenesis.
- Fracture porosity, which is caused by stress following deposition.

The above three forms of porosity create a very complex path of fluids and directly affecting well producibility.

Carbonate Evaluation

Exploration and evaluation programs for carbonates are similar to those for sandstone reservoirs. However, new tools, techniques, and interpretation methodologies are required to address the specific challenges above to drill and produce these reservoirs optimally.

The relationship between formation permeability and porosity is relatively simple for a sandstone reservoir. In contrast, most of carbonate reservoirs exhibit several trends of permeability/porosity correlation depending on the pore size distribution and texture (Figure 5).

Any attempt to calculate the total hydrocarbon content of a carbonate reservoir will be hampered by porosity variations. In order to estimate how much oil can be produced (recoverable oil), geologists and engineers must understand the porosity distribution, fluid saturation, and extent to which pores are linked together in order to allow fluid flow. Large scale porosity heterogeneity present a major challenge to the oil industry.

Presence of hydrocarbon is not always correlatable with conventional open hole logging data especially in heterogeneous carbonate reservoirs. In carbonate reservoir with inherent azimuthal anisotropy, it is observed very often that the hydrocarbon production is inconsistent with total porosity measurement.

LWD Technology used in South Fuwaris Field

Most of the field lateral holes are drilled using the following LWD technology:

- Distance to boundary technology which is used to place the well trajectory in the sweet spot of the reservoir.
- Azimuthal Density Neutron technology which is used to evaluate formation porosity and saturation in combination with resistivity.
- Azimuthal resistivity Imaging which is used for both true formation resistivity and borehole imaging.

Evaluating carbonate reservoirs often requires a combination of data gathering and interpretation techniques to help in predicting permeability and fluid flow behavior. LWD electrical imaging can play a big role in achieving this task.

Imaging with LWD

Logging While Drilling (LWD) technology can produce several images while drilling as follows:

- Azimuthal GR image
- Azimuthal Density image
- Azimuthal PEF image
- Azimuthal Caliper image
- Azimuthal Resistivity image

The above images have the advantages of full borehole coverage since LWD tools are always under rotation conditions when using rotary steerable drilling technique. The main difference between the images is the vertical resolution. Density and PEF images have a vertical resolution of around 6 inches. They are useful for structural interpretation and formation dip determination during Geosteering. Resistivity images are usually of higher vertical resolution (around 0.2 inches) therefore it is more suitable for borehole delayed analysis like texture and heterogeneity. Please refer to Figure 6 for the LWD images resolution comparison

Resistivity Imaging with LWD

The LWD resistivity imaging tool plays the role of two different tools, a laterolog resistivity measurement and a borehole resistivity imaging (Figure 7). The imaging capability of the LWD tool can produce several images with different depths of investigation. This is rather useful especially if borehole break out is encountered. In this case, the shallow image will be more affected by borehole break out while the deep image will be more sensitive to formation characteristics such as bedding, fractures and vuggy porosity (Figure 8). The imaging capability also provides a high resolution image that can play a big role in carbonate texture evaluation (Figure 9 and Figure 10).

Several experiments were made to compare the image quality obtained by LWD technology to the conventional wireline imaging. The results were showing a very good match between the two images. Moreover, sometimes LWD images are showing more details than conventional wireline images since it was acquired while drilling before any hole shape deterioration takes place (Figure 11).

Workflow and Methodology

A workflow has been developed to characterize and quantify secondary porosity and hence permeability profile from LWD images; Figure 12 illustrates the workflow. The workflow starts with the image processing and manual dip picking in order to get basic structural interpretation.

The secondary porosity is computed using Porosity Spectrum analysis algorithm (PoroSpec) from the processed image and considering the formation dip orientation. Finally, an image derived permeability profile can be calculated by applying porosity to permeability transform. And last, different flow units along the borehole trajectory can be obtained by combining secondary porosity, image-derived permeability and open hole conventional logging data.

Transformation from Resistivity to Porosity Image

Calibrated electrical images from the formation microimaging tools are essentially a conductivity map of the borehole wall, primarily from within the flushed zone. The classic Archie saturation equation in the flushed zone is:

$$S_{xo}^{n} = \frac{aR_{mf}}{\Phi^{m} R_{xo}}$$

By setting Sxo = 1.0 , a = 1.0 and m = n = 2.0 , the LWD resitivity images can be transformed into a porosity map using the equation below:

$$\Phi = \sqrt{\frac{R_{mf}}{R_{xo}}}$$

A reasonably accurate value for mud filtrate resistivity, Rmf, is usually available and the flushed zone resistivity, Rxo, is the numerical value of the electrical image at any particular point (Newberry et al., 1996).

By statistically examining the distribution of porosity over a short vertical window (1.2 in.), it is possible to locate the porosity value that separates the matrix porosity fraction from that of the secondary porosity in that local region. It is then possible to count the sections that contribute to primary porosity and those that contribute to secondary porosity. Summing the primary and secondary components then yields the total porosity.

For intervals having homogeneous porosity the comparison to neutron/density logs is normally excellent. However, there is often little correlation over zones having a heterogeneous distribution of porosities. This discrepancy is due to the fact that the nuclear measurements are highly azimuthal in nature, whereas the PoroSpect results are derived from data which covers most of the circumference of the borehole thereby providing a more consistent answer.

The Technique

Schlumberger has introduced a new approach to utilize borehole electrical images to analyze the complex porosity system in carbonate reservoirs. Through this technique porosity distribution and quantity of vug fraction can be obtained. The primary assumption for this technique is that the resistivity data from the electrical images are measured in the flushed zone of the borehole.

The electrical images can then be transformed into a porosity map of the borehole after their calibration with the shallow resistivity and log porosity (preferably effective porosity). Automated analysis of this porosity map, windowed over short intervals, provides a continuous output of the primary and secondary porosity components. At every specified sampling rate (generally 0.6 inch), porosity distribution histograms are computed.

The homogeneous carbonate intervals give unimodal distribution (Figure 13). In vuggy carbonates, bimodal distribution of porosity is observed (Figure 14). While in the most heterogeneous carbonates where cementation, primary porosity and vuggy porosity are present, trimodal porosity distribution may be observed (Figure 15). On such histograms, the points from the high porosity tails represent vug and fracture fractions of porosity and the points from the low porosity tails belong to the dense or cemented areas of the host rock.

Across the homogeneous carbonate intervals, which compute unimodal porosity distribution, the average of the image porosity reads nearly the same as the effective log porosity. While the unimodal porosity distribution changes into bimodal or trimodal distribution across the heterogeneous carbonate intervals. The average image porosity across such intervals may be either more or less than the effective log porosity depending upon type of heterogeneity, i.e. vugs, molds, fractures or matrix patches of very high porosity or dense areas with low porosity.

Through iterative experimentation, the core permeability exponentially varied with vug porosity as follows:

$$k = a\phi^2 \times 10^{b\phi_{vug}}$$

Where **φ** and **φvug** are the total porosity and vug porosity from borehole image porosity processing, respectively, and **a** and **b** are constants. The **aφ 2** term is equivalent to permeability in homogeneous rocks (when vug porosity is zero).

The constant **a** was determined by matching **aφ 2** to the formation permeability in intervals with negligible vug porosity. In vuggy zones, the permeability is dominantly controlled by the vug porosity (i.e. the exponential term above). Note that the two constants **a** and **b** may be unique for a particular oil field with its uniquely characteristic pore system, vug connectivity, and fluid content (i.e. the nature of the geological heterogeneity and its corresponding log response may be unique).

LWD Imaging for Sabriyah Wells

The above technique was used for the first time in the Sabriyah Field. The borehole resistivity image was first processed for structural dips. This step was followed by porosity spectrum analysis in order to quantify the amount of secondary porosity. The formation permeability profile was estimated qualitatively from both total porosity and secondary porosity. Figure 16 shows the typical display of the processing.

In Figure 17 is a typical field display illustrating the different measurements that were obtained in real time while drilling a typical well as follows:

- Track # 1: GR / ROP
- Track # 2: Electromagnetic Resistivity
- Track # 3: Density / Neutron / PEF
- Track # 4: Resistivity image map
- Track # 5: Density image map

Figures 18, 19 and 20 are showing some of the snap shots of the processed results as follows:

- Track # 1: Static processed image
- Track # 2: Dip picking
- Track # 3: Dynamic processed image
- Track # 4: Image porosity – vs – density / neutron cross plot porosity
- Track # 5: Secondary porosity
- Track # 6: Porosity histogram
- Track # 7: Formation permeability calibrated to Stethoscope permeability (red dots)
- Track # 8,9,10: Connectivity analysis

Conclusions

In addition to core analysis, different logging tools and methodologies are employed in the oil industry to identify facies types. Borehole imaging is one of them. The above technique gives a quantified representation of the internal organization or rock fabric in the form of continuous log curves. Using a set of these curves as discriminators, a facies model can be generated. To make it more realistic, the facies model can be defined by calibrating with cores. Once a facies model is generated, an artificial neural network is designed. The net is then trained over the cored interval. The trained net can then be used to estimate facies assemblage in the remaining part of the well where cores are not present. Moving a step ahead, the trained net can be used to estimate facies assemblage in wells within the same geological domain.

Porosity heterogeneities within carbonates are common and can cause the potential of a reservoir sequence to be incorrectly evaluated if only standard log and core evaluation approaches are adapted. High resolution electrical images directly defining the rock type thus provides valuable information about decimeter-scale carbonate heterogeneities and porosity fabrics. Moreover, the heterogeneous nature of the porosity and the rock type are extracted using specialized image texture algorithms. These have been developed to automatically highlight geological features such as vugs and patches. The internal geometry of the formation is particularly important, as it is a major factor which influences the fluid flow and recovery efficiency in a carbonate reservoir. Quantification of borehole electrical images for porosity analysis in heterogeneous carbonate reservoir may lead to more realistic reserve estimation. Thus, it forms a vital step in the workflow of a reservoir optimization process.

Acknowledgement

The authors would like to thank KOC management for allowing to publish this material and for believing in the latest LWD technology.

Selected References

Bahukhandi, Yogesh, U.C. Bhat, Somenath Kar, Chandan Majumdar, and Dipanka Behari 2011, Flow unit characterization aided by quantified secondary porosity result from high resolution LWD images in heterogeneous carbonate reservoir; A novel approach: IPTC 14772, November 15-17, Bangkok, Thailand.

Newberry, B.M., L.M. Grace, and D.D. Stief, 1996, Analysis of carbonate dual porosity systems from borehole electrical images: SPE 35158 presented at the Permian Basin Oil and Gas Recovery conference, March 27-29, 1996.

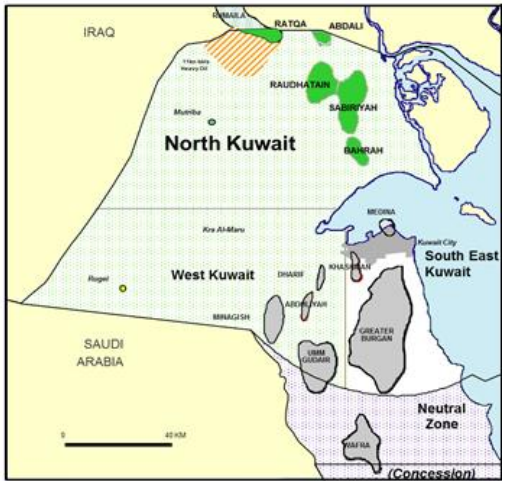

Figure 1. Sabriya location map.

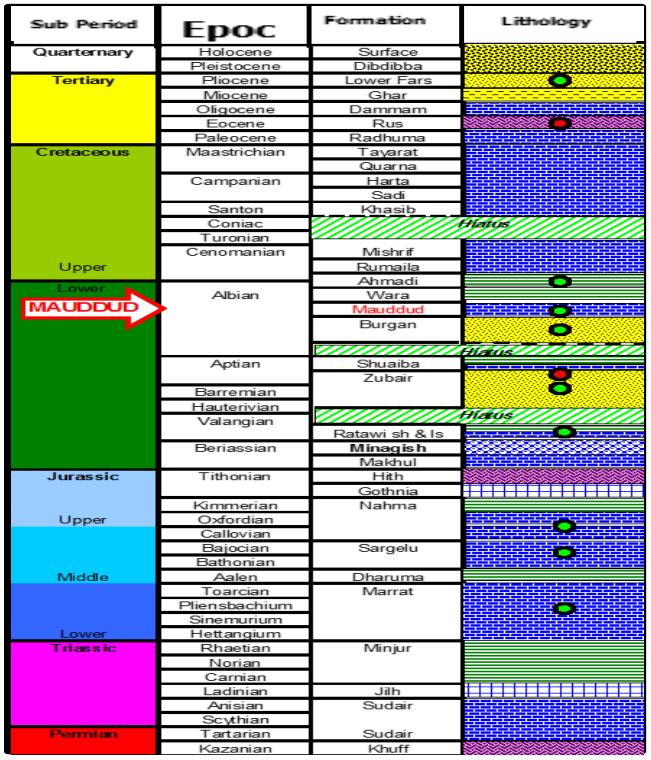

Figure 2. Strategraphic column.

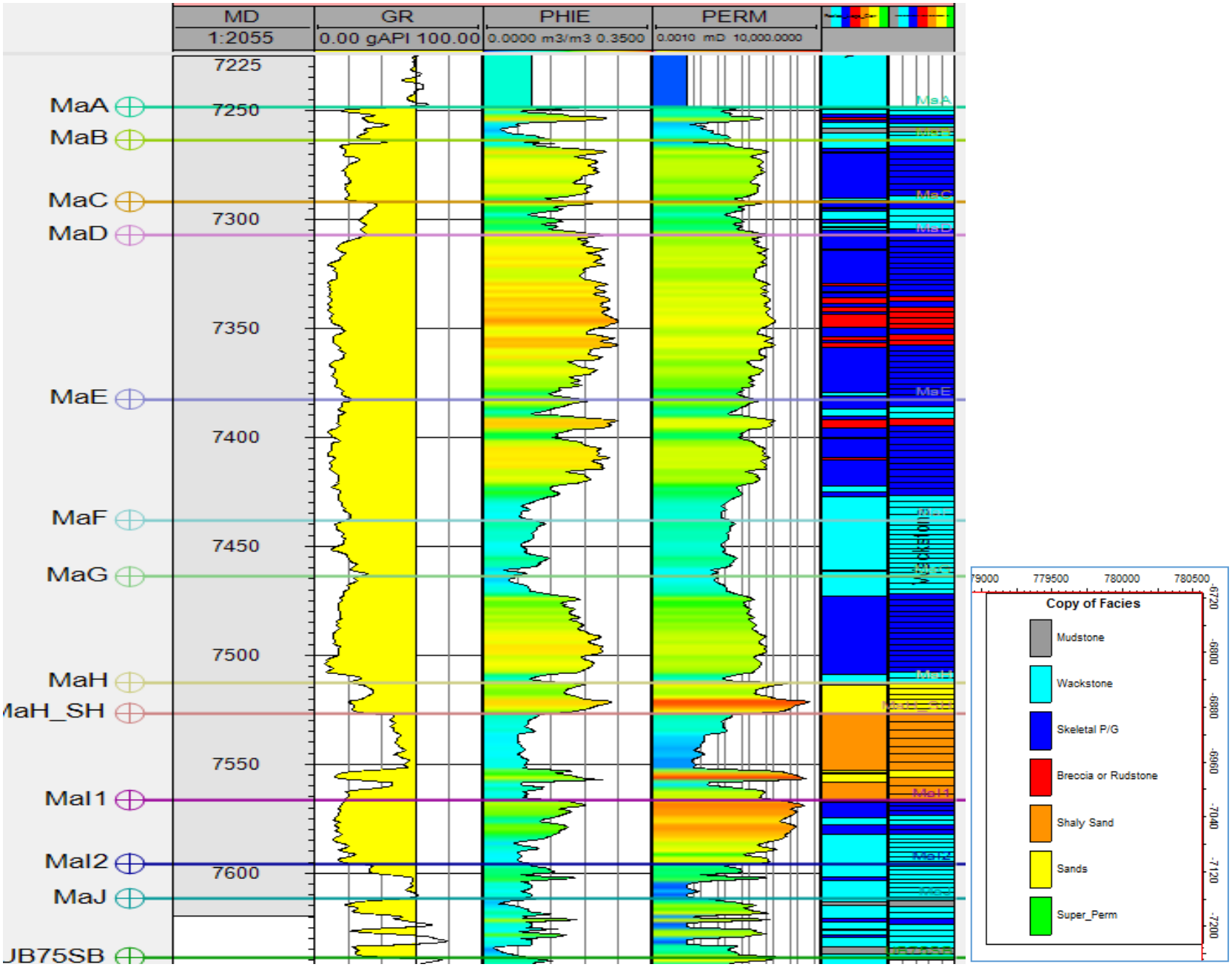

Figure 3. Depositional facies example.

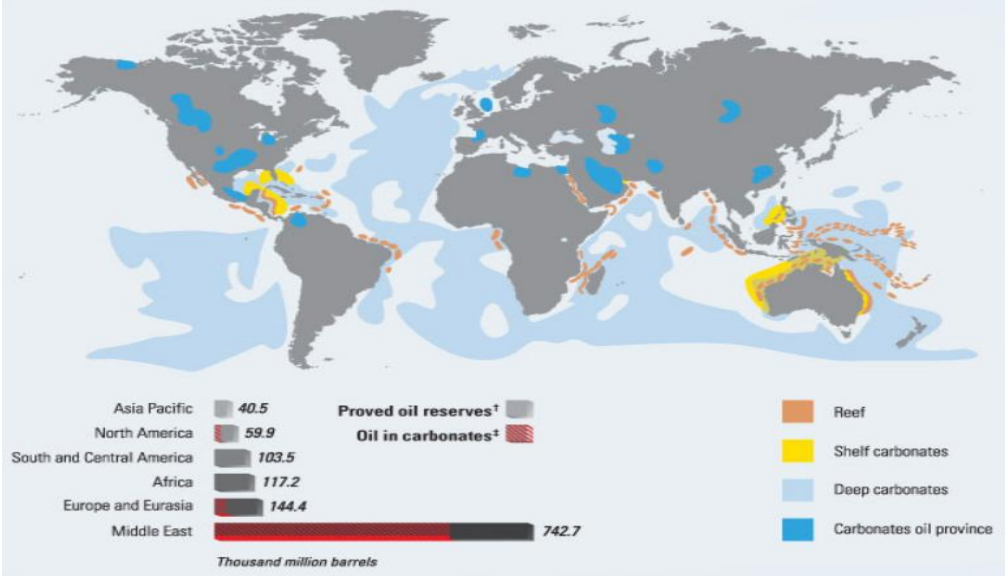

Figure 4. Carbonate reservoir distribution around the world.

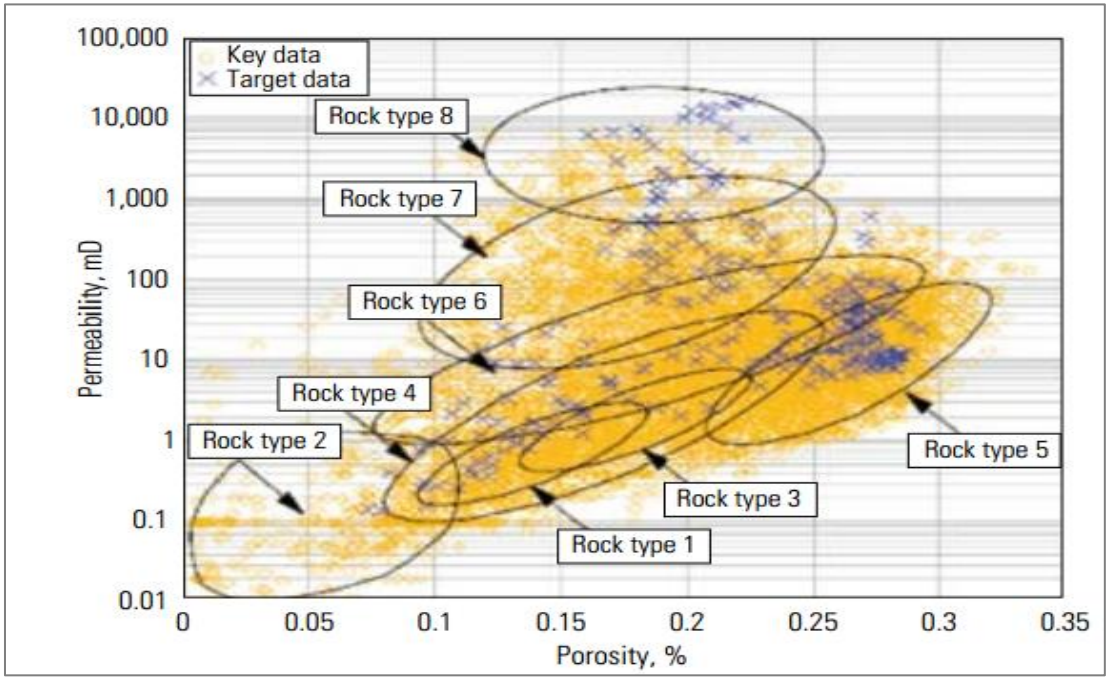

Figure 5. Carbonate rock types as defined in terms of the relationship between their porosity and permeability.

Figure 6. Vertical resolution for different imaging techniques of LWD tools.

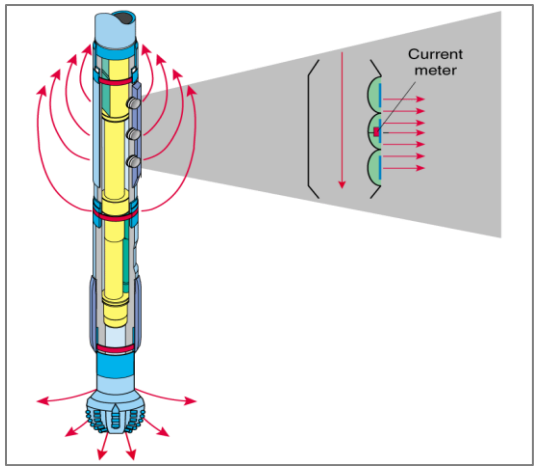

Figure 7. Different measurements from a Laterolog type LWD technology.

Figure 8. Different images obtained by LWD technology with different depth of investigation.

Figure 9. High resolution sensor for resistivity imaging with LWD.

MicroScope standard Image Resolution	
Button Size	1" vertical, 0.6" horizontal
Vertical Resolution	1"
Horizontal Resolution	0.6"
Pixel Size	0.3" vertical * 0.35" Horizontal
# Azimuthal Bins	56

MicroScope HD Image Resolution	
Button Size	0.4" diameter
Vertical Resolution	0.4"
Horizontal Resolution	0.4"
Pixel Size	0.2“ * 0.125"
# Azimuthal Bins	160

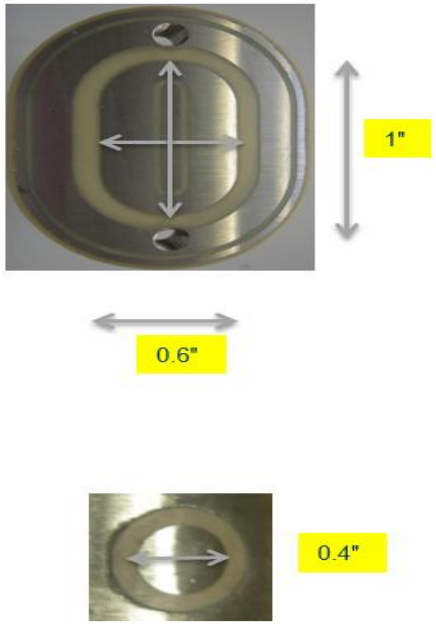

Figure 10. Comparison of the vertical resolution of different LWD technologies.

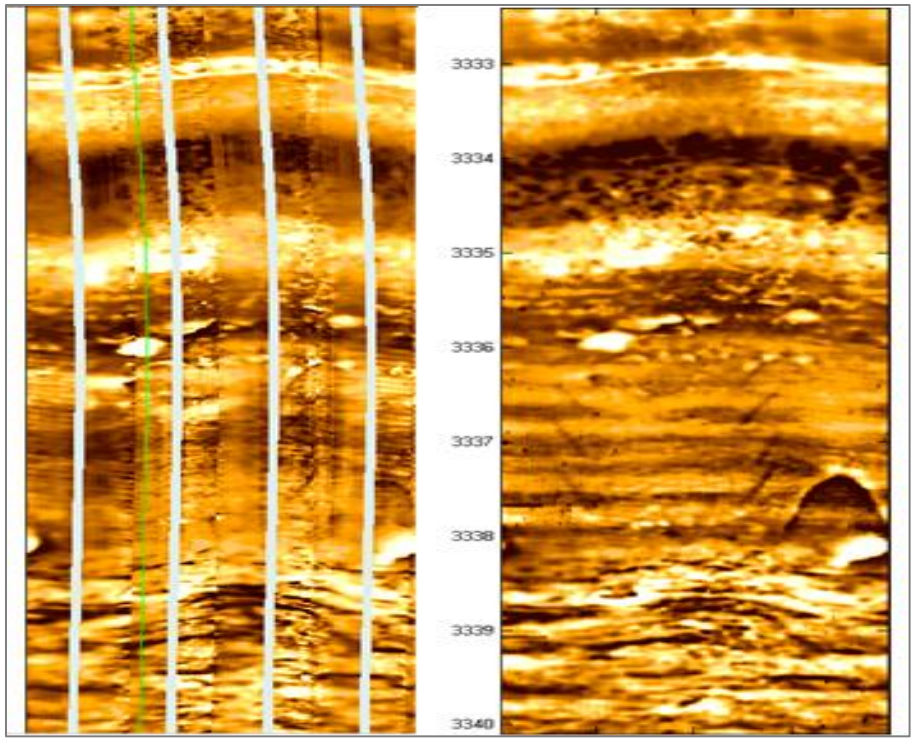

Figure 11. Comparison of imaging with Wireline technology vs LWD technology.

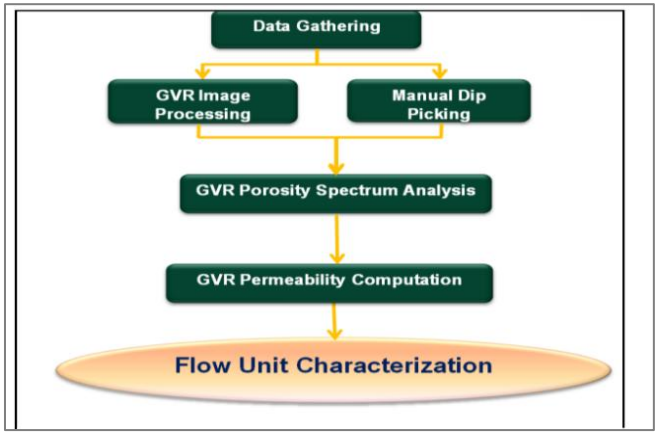

Figure 12. Workflow for flow unit characterisation from LWD images.

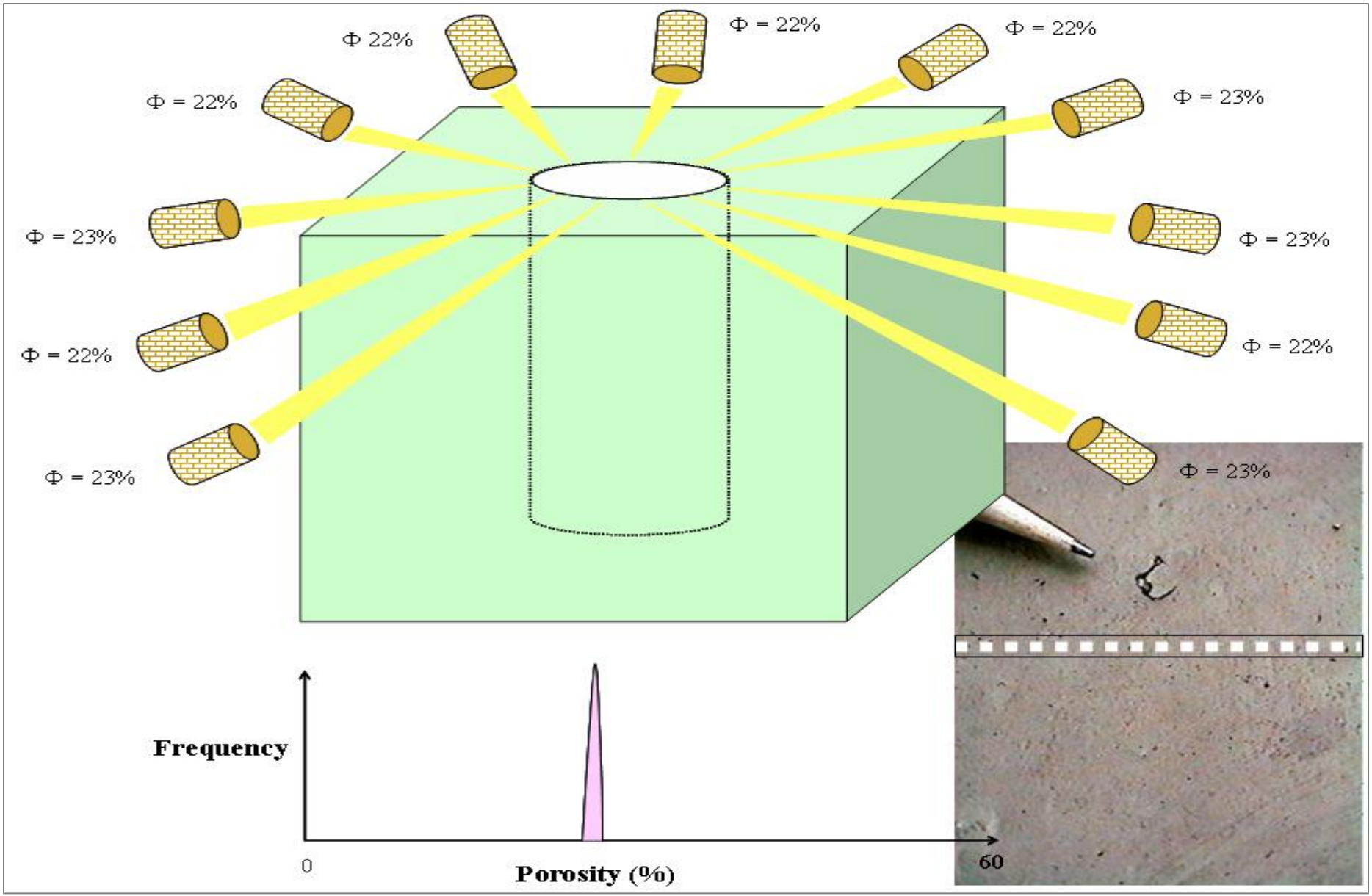

Figure 13. Porosity histogram of a homogeneous carbonate rock.

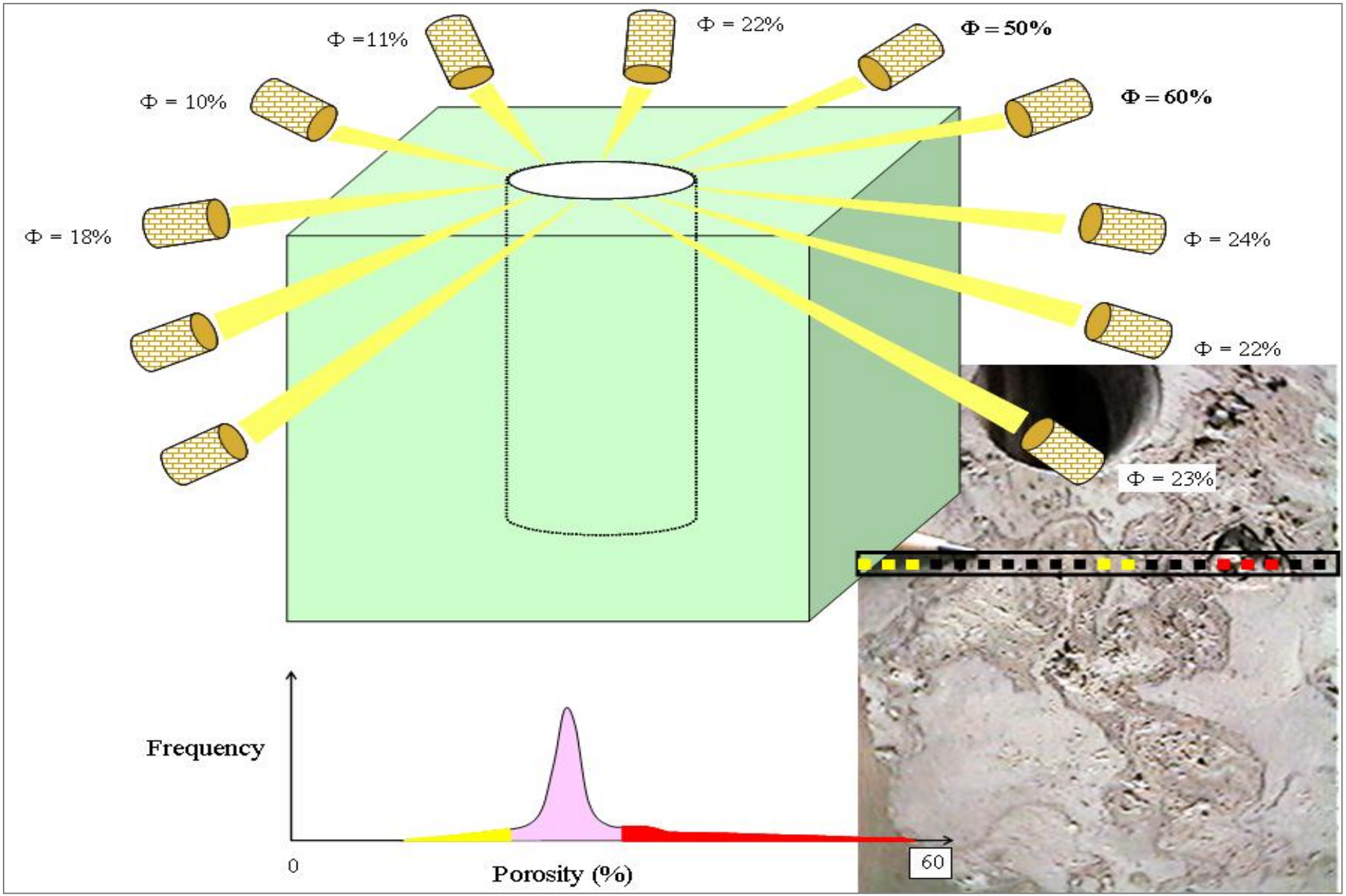

Figure 14. Porosity histogram of a heterogeneous carbonate rock.

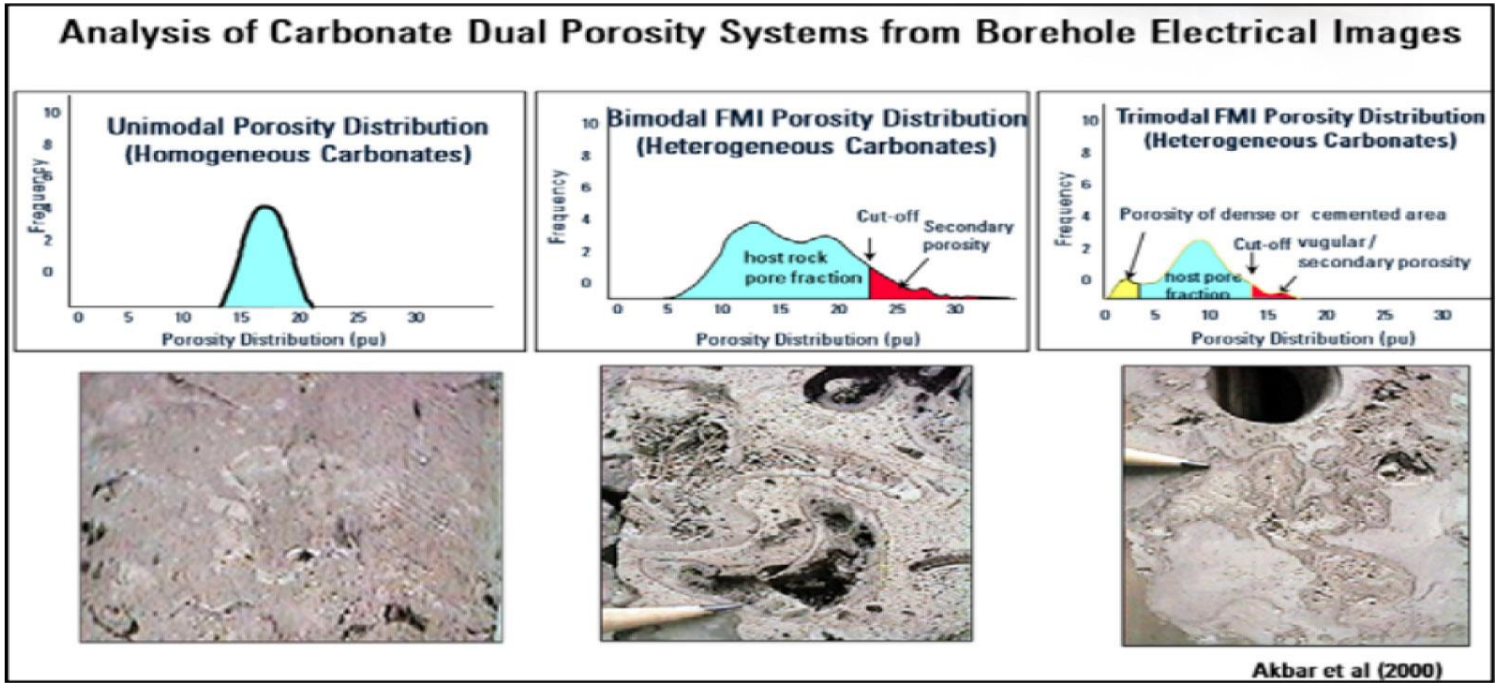

Figure 15. Carbonate dual porosity distribution.

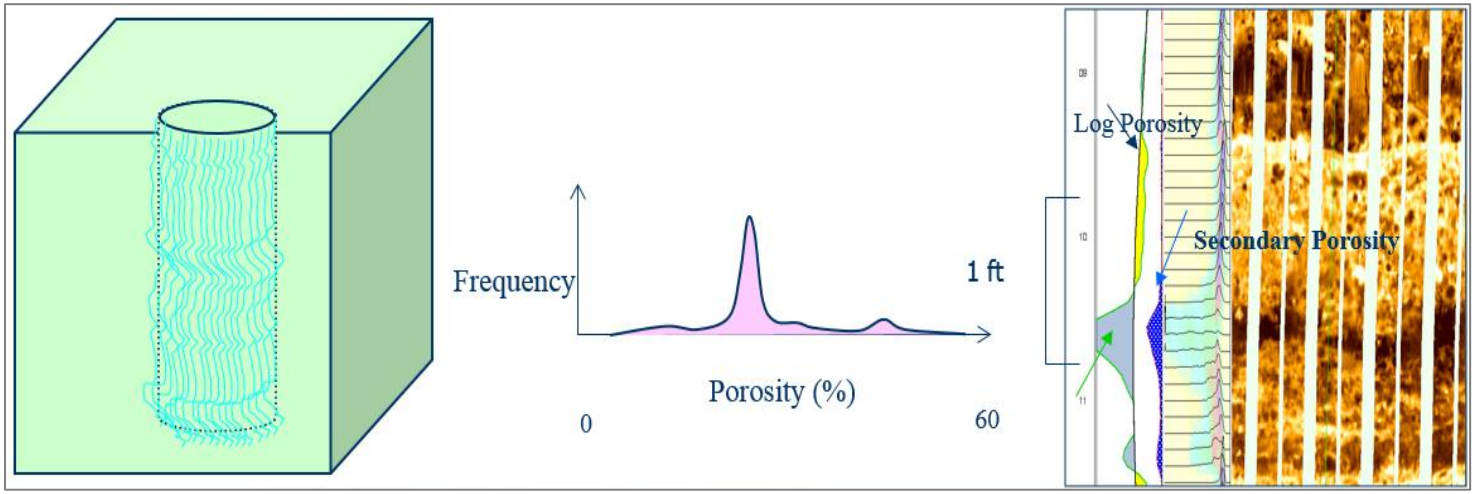

Figure 16. Porosity spectrum analysis typical display.

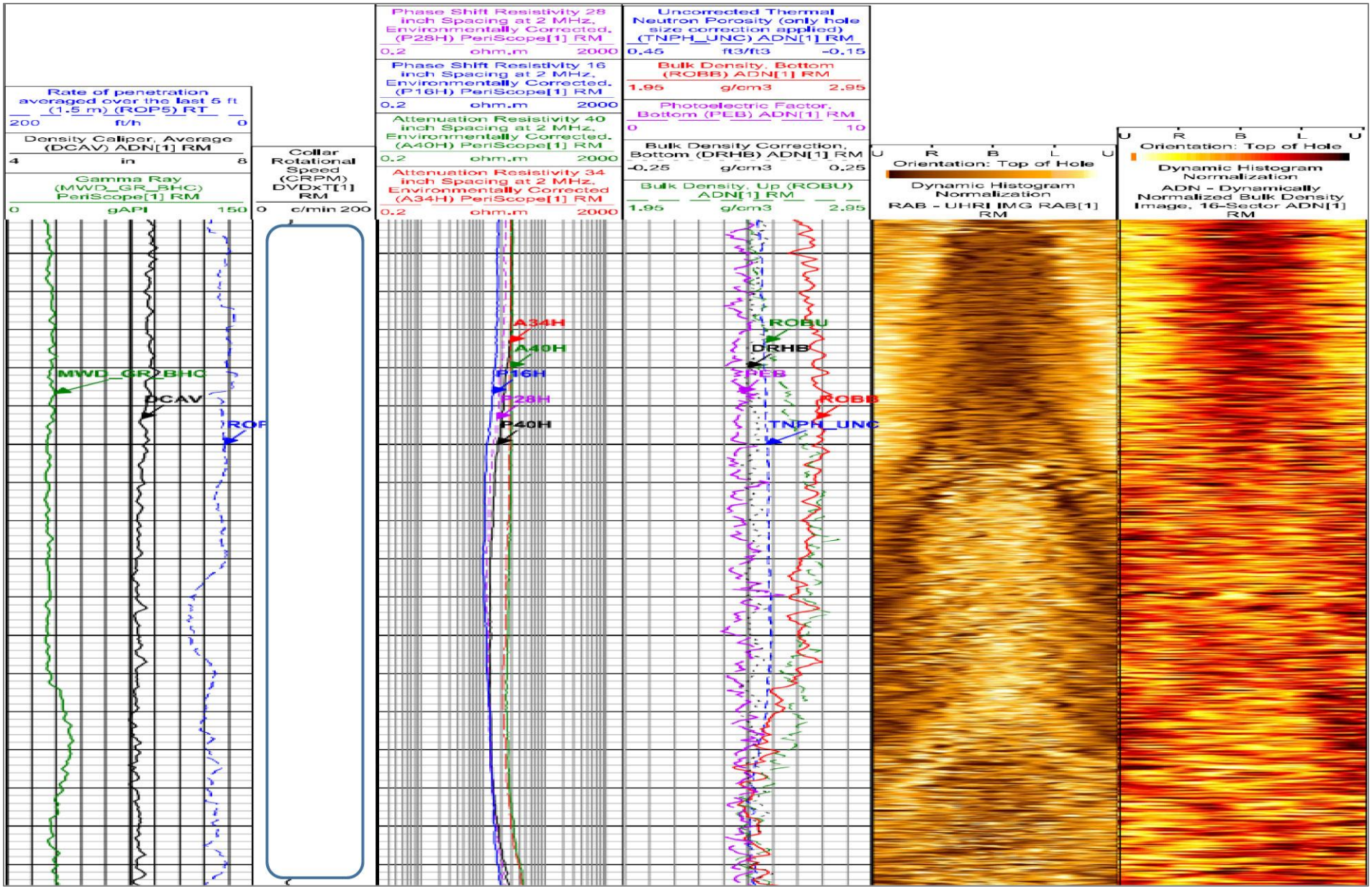

Figure 17. Acquisition display showing both resistivity image and density image.

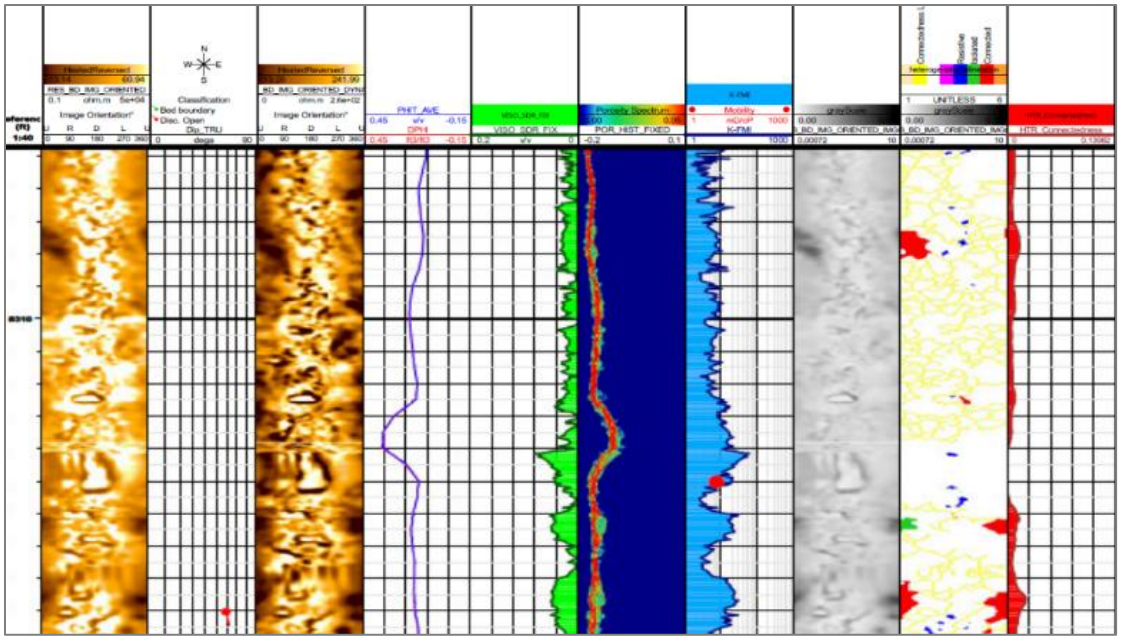

Figure 18. Porosity spectrum processing results showing secondary porosity and permeability.

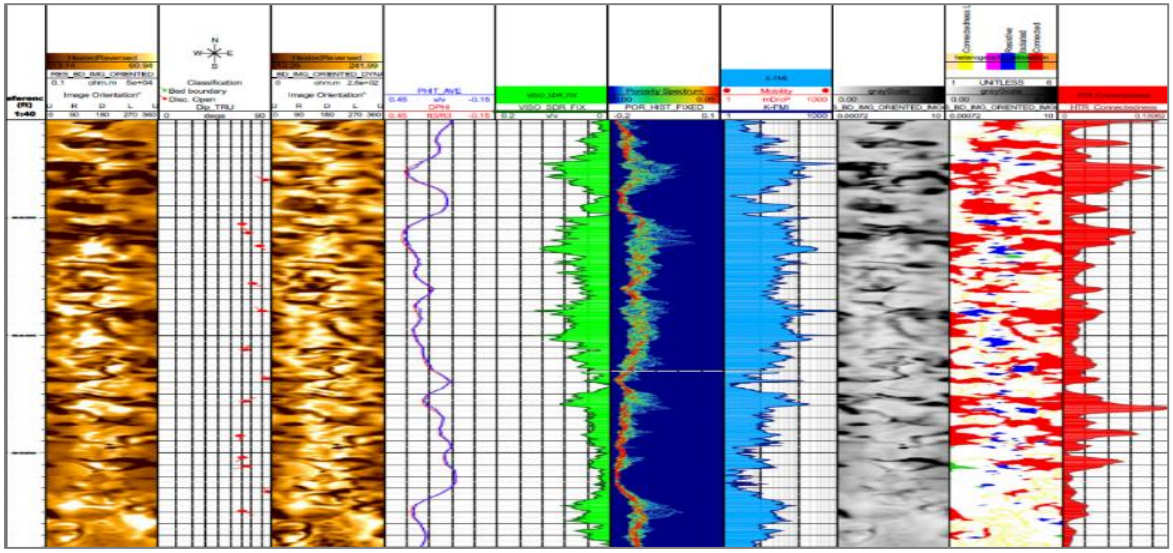

Figure 19. Porosity spectrum processing results showing secondary porosity, permeability and some fractures.

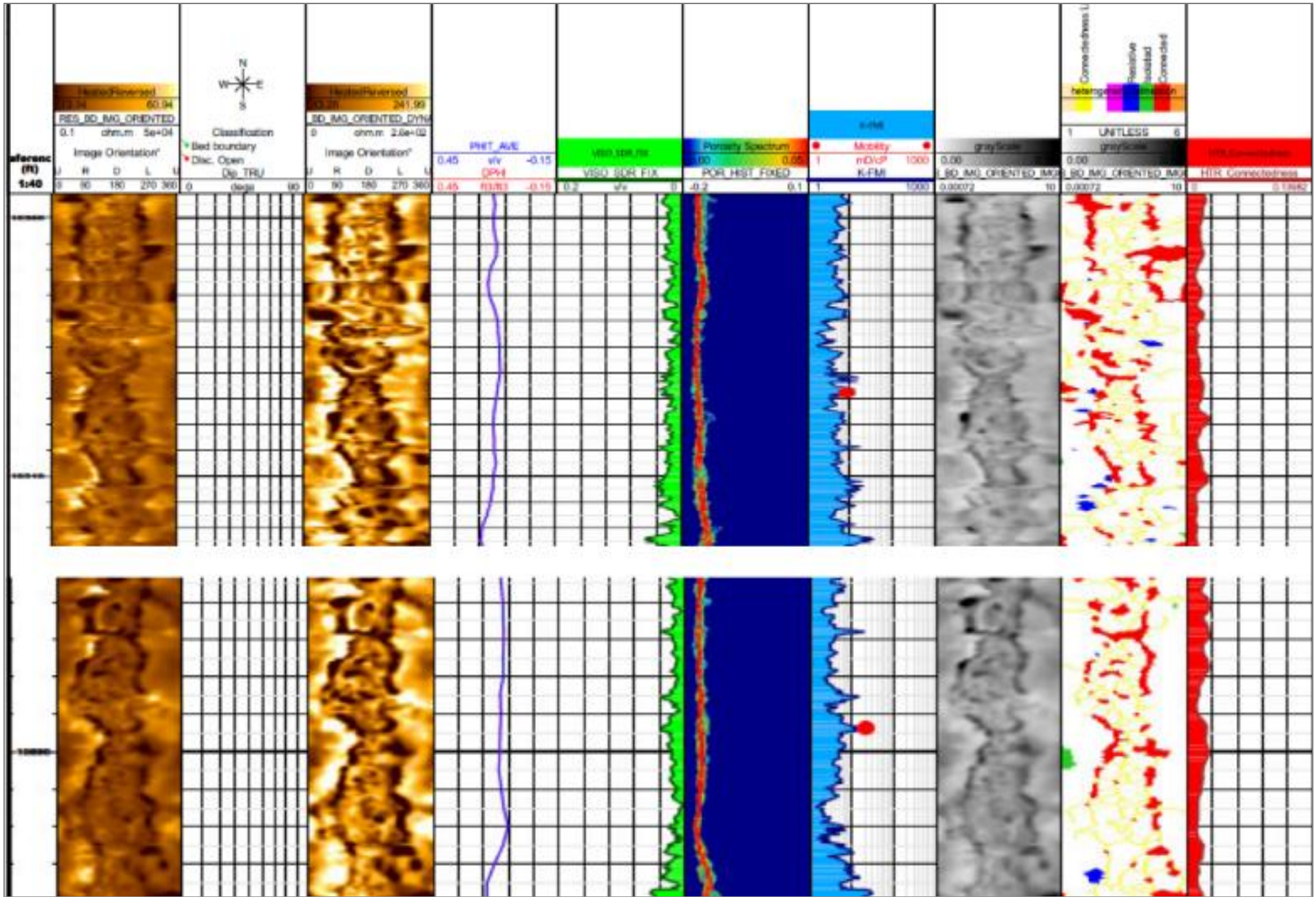

Figure 20. Porosity spectrum processing results and a comparison with mobility from formation pressure while drilling results.